

Chapter 5

Phase Shifter Measurements

5.1 : Introduction

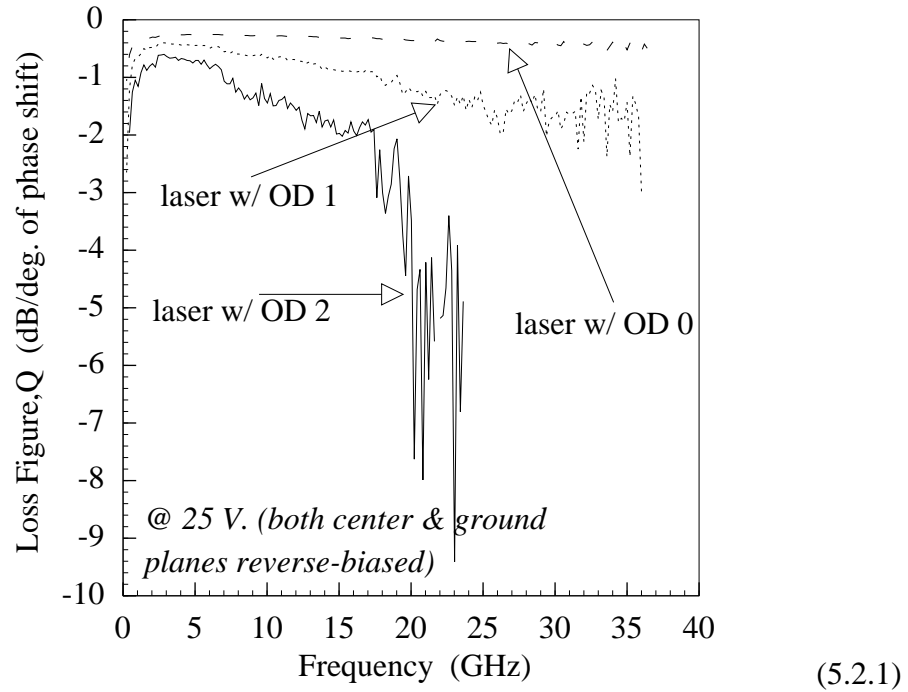
The application of co-planar waveguide (CPW) as an optically-controlled phase shifter or resonator has previously been demonstrated [Cheung et al. 1989; Islam et al. 1990]. The various issues evolved in the operation of the Schottky-contacted CPW phase shifter are described by an accurate equivalent circuit model, discussed in Chapter 3 and Chapter 4. In this Chapter, a systematic investigation of the controlling mechanisms of a CPW phase shifter is presented. Furthermore, experimental results from various phase shifters are discussed in detail. Experimental results of epitaxially lifted-off devices on a transparent quartz substrate are also discussed. Preliminary results on the response times of the phase shifter to pulsed illumination are also discussed at the end of this Chapter.

For actual devices, prior to any high frequency phase shifting measurement, the devices are examined in terms of DC current - voltage (I-V) and low frequency capacitance - voltage (C-V) measurements. DC I-V measurements were used to verify good Schottky contact between the deposited electrodes (both center conductor and ground planes) and the epi GaAs. Low frequency capacitance values are measured as a function of voltage and frequency, and are compared with values predicted by the model described in Chapter 4. After DC and low frequency measurement, S-parameter values are obtained from high-frequency measurements. These values are used to describe phase shifting properties along with related parameters, such as insertion loss, effective dielectric constant, and characteristic impedance. Bias-controlled measurements are done first, and at the proper bias point, optical-control measurements are performed. The proper bias point is found at the bias voltage which exhibits the lowest insertion loss per degree of phase shift at different optical intensities. Optical sources used as the controlling mechanism were a broadband microscope illuminator, a laser at a wavelength of 709 nm, and a

red encapsulated LED, all of which emit photons with energies higher than that of the GaAs bandgap energy. Variations in optical intensities when using lasers were provided with different neutral density filters. All measurements were done with HP 8510B Automatic Network Analyzer in conjunction with rf wafer probes. Probing was done with Design Technique's Ground-Signal-Ground microwave probes. Phase shifting performance is presented as insertion loss per degree of phase shift, referred to as the loss figure, against frequency of operation. The lower the magnitude of this loss figure, the better is phase shifting capabilities of a device from a practical consideration. Another important point for practical implementation of these phase shifters is the response time of these devices, which is also discussed in this Chapter, where preliminary results on the time-dependent pulse propagation is presented.

5.2 : Voltage-controlled phase shifters

The most important performance parameter for a voltage-controlled phase shifter can be defined as "Loss Figure", which represents the total insertion loss per degree of phase shift. Here, a reference voltage is chosen and the phase shift between this reference voltage, V_{ref} and the operating voltage, V_{max} is calculated to get the total phase shift, whereas the insertion loss is the maximum total insertion loss corresponds to the operating voltage, V_{max} . Mathematically, loss figure (LF) is defined as



where IL and ϕ correspond to insertion loss and total phase respectively. The reference voltage is chosen where insertion loss is the minimum, which is the case with full depletion of the top epitaxial layer. Alternatively for this performance index, sometimes change in insertion loss is considered instead of the total insertion loss, where LF can be defined as

done are shown in Fig. 5.1(a), (b) and (c). In Fig. 5.1(a), the center conductor is reverse biased with respect to the ground planes, whereas Fig. 5.1(b) shows ground planes reverse biased with respect to the center conductor. Fig. 5.1(c) shows the biasing where both center conductor and ground planes are reverse biased with respect to the separate ohmic contact.

Fig. 5.1: Three biasing conditions employed in the phase shifter measurements. (a) Center conductor reverse biased with respect to the ground planes; (b) Ground planes reverse biased with respect to center conductor and (c) Both ground planes and center conductor reverse biased with a separate ohmic contact.

By changing the bias voltages applied to the Schottky-contacted signal and ground lines, phase constants and attenuation of the devices can be varied. At zero bias, the device, which is basically a long distributed transmission line (1 cm long), usually is very lossy because the active region of this device is an MBE grown lightly-doped epitaxial GaAs layer. With a reverse bias applied to either center conductor, ground planes, or both, the lossy epi-layers start to deplete, which reduces the insertion loss of the device and changes the phase constant of the line. For most devices investigated, with an n-type carrier concentration in the epi-layer in the mid- $10^{15}/\text{cm}^3$, the zero-bias insertion loss above 10 GHz becomes less than -50 dB (for a device 1 cm long) which is in the noise level of the measuring equipment (HP 8510B Automatic Network Analyzer). Therefore, for low voltage cases, it was not possible to measure the loss per degree of phase shift (loss figure) at frequencies above 10 GHz, as both phase and loss are in the noise levels. At higher frequencies, the magnitude of loss figure tends to increase in most cases, the reason being the difference in effective indices of refraction ($n_{\text{eff}} = \beta/\beta_0$) between the reference and measured bias points becomes smaller, while the difference between insertion losses remain more or less same. This is shown in Fig. 5.2(a) and (b), where insertion loss and n_{eff} are shown against frequency for different bias conditions on the sample #1675c. For all cases, the loss figures turn out to be best for zero voltage bias when full depletion voltage is

Fig. 5.2(a) : Change of insertion loss at different bias voltages. All voltages correspond to ground planes reverse-biased with respect to center conductor. Measurements are done on #1675c sample.

considered as the reference point. Intermediate voltages with the same reference point provide worse performance and with a voltage very close to the reference voltage performance is the worst.

Sample #1675c has a 3 μm epitaxial GaAs layer, with an n-type doping concentration of $\sim 5 \times 10^{15} / \text{cm}^3$, sitting on the top of 1000 \AA of undoped AlAs (sacrificial layer for epitaxial lift off) on top of a semi-insulating GaAs substrate.

Fig. 5.2(b) : Change of effective index of refraction (n_{eff}) at different bias voltages. All voltages correspond to ground planes reverse-biased with respect to center conductor. Measurements are done on #1675c sample.

Fig. 5.3 : Performance of a bias-dependent phase shifter (in terms of dB loss per degree of phase shift) when ground planes are reverse-biased with respect to center conductor. Reference voltage is taken as 30 volts. Measurements are taken on #1675c sample.

Fig. 5.4 : Performance of a bias-dependent phase shifter (in terms of dB loss per degree of phase shift) when center conductor is reverse-biased with respect to ground planes. Reference voltage is taken as 30 volts. Measurements are taken on #1675c sample.

Fig. 5.5 : Performance of a bias-dependent phase shifter (in terms of dB loss per degree of phase shift) when both center conductor and ground planes are reverse-biased with respect to a separate ohmic contact. Reference voltage is taken as 30 volts, which is the full depletion bias condition. Measurements are taken on #1675c sample.

Fig. 5.6 : Performance of a bias-dependent phase shifter (in terms of dB loss per degree of phase shift) before (on GaAs) and after Epitaxial Lift off (on Quartz); when both center conductor and ground planes are reverse-biased with respect to a separate ohmic contact. Reference voltage is taken as 25 volts. Measurements are taken on #1675c sample.

Figure 5.3 shows the variation of loss figure with the frequency of operation when the ground planes are reverse biased with respect to the center conductor (i.e., positive voltage is applied to the center conductor which actually means that the center conductor is slightly forward biased as discussed in Chapter 4). The reference voltage considered is 30 volts, which is the full depletion voltage for this sample. The performances at three other voltages are compared with each other, where a 0 volt loss figure turns out to be the best, at least up to 10 GHz. Fig. 5.4 and 5.5 show similar variation of loss figures, when the center is reverse biased with respect to ground planes and both ground planes and center conductor reverse biased simultaneously with respect to the separate ohmic contact on the sample, respectively. For both cases, 25 volt bias performance was the worst while 0 volt performed the best. Similar comparisons are made after the sample is epitaxially lifted-off (ELO) from its parent semi-insulating GaAs and put onto a transparent quartz substrate. In this case 25 volts is taken as reference point, and loss figure is measured for 0 volt bias case both before and after ELO, which is shown in Fig. 5.6. Loss figure after ELO shows a better performance, and probably gives the best of all bias-controlled performances up to 10 GHz.

The performance index of loss figure is also indicative of the required length to make a 180 degree phase shifter at varying frequencies. Figure 5.7 shows the variation of required length (for a 180 degree phase shifter) for three different bias conditions when ground planes are reverse biased with respect to center conductor. Similar variation is shown for before and after ELO cases at zero voltage, as shown in Fig. 5.8. The smaller the length becomes, the device loses its

properties as a "distributed" transmission line and eventually becomes a "lumped" circuit element and hence works as a conventional Schottky diode.

Fig. 5.7 : Length required for a bias-dependent phase shifter to produce 180° phase shift, when ground planes are reverse-biased with respect to center conductor. Reference voltage is taken as 30 volts, which is the full depletion bias condition. Measurements are taken on #1675c sample.

Fig. 5.8 : Length required for a bias-dependent phase shifter to produce 180° phase shift before (on GaAs) and after Epitaxial Lift off (on Quartz); when both center conductor and ground planes are reverse-biased with respect to a separate ohmic contact. Reference voltage is taken as 25 volts. All measurements are taken on #1675c sample.

The similar dependence is shown with another sample, which has $2\ \mu\text{m}$ of epitaxial layer of GaAs with mid $10^{15}\ \text{cm}^{-3}$ concentration (labeled as #2299a) in Figs. 5.9 and 5.10. As these data are for a sample with similar doping but smaller thickness of lossy epi layer, the bias dependence and hence the full depletion occurs at a much lower voltage. The bias dependences are consistent with doping concentrations and thicknesses even from a simple one dimensional depletion approximation, when an appropriate model is chosen. This is discussed in detail in Chapter 4. Figure 5.9 shows the variation of loss figure at three different bias voltages when ground planes are reverse biased with respect to the center conductor. The reference voltage is taken as 8 volts, which is the full depletion voltage. Figure 5.10 shows similar variation for center conductor reverse biased with respect to ground planes. For both cases, the loss figure is best for zero bias situations. As frequency is increased, the loss figures get worse for center conductor bias conditions, compared to the ground plane bias conditions.

Fig. 5.9 : Performance of a bias-dependent phase shifter (in terms of dB loss per degree of phase shift) when ground planes are reverse-biased with respect to

center conductor. Reference voltage is taken as 8 volts, which is the full depletion bias condition. Measurements are taken on #2299a sample.

Before discussing the experimental measurements by optical control, it is necessary to define the performance index of the phase shifter, "Loss Figure". Loss figure for an optically-controlled phase shifter has two variables, one being the fixed dc "reference" bias, V_{ref} and the other one, the variable optical intensity. Therefore, mathematically loss figure can be expressed as

$$(5.3.1)$$

where, IL and ϕ stand for insertion loss and phase angle respectively. I_{max} is the maximum illuminating intensity used for the optically-controlled phase shifter.

Optical experiments were performed on four different samples (#1229, #1675c, #1946a and #2299a). Sample #1229 has 2 μm of $\sim 7 \times 10^{15}$ n-type epi layer on the top of 500 \AA of AlAs (sacrificial layer for ELO) on a semi-insulating (SI) GaAs substrate. After ELO, 2 μm of same epi layer sits on the top of a quartz (pyrex) substrate. The metallization scheme for the sample is 300 \AA of chrome followed by 1.2 μm of evaporated silver. For the doping concentration and layer thickness used for this sample, a dc reverse bias of 20 V applied to the ground plane conductors produced maximum sensitivity. The device was illuminated with a laser diode operating at 809 nm. Typical intensity at the sample surface was 0.65 mW/cm^2 . DC current-voltage measurements (I-V) taken before and after ELO gave nearly identical results. However, under both unilluminated and illuminated conditions, the high frequency characteristics after ELO showed a large decrease in insertion loss and increase in optically induced phase shift, compared to that measured before ELO, as shown in Fig. 5.11 and 5.12. In general, the device performance before lift off is worse than for a comparable n⁻ GaAs epitaxial layer grown directly on a semi insulating (SI) substrate without the intervening AlAs layer. This is primarily due to a difference in band bending at the bottom surface of the GaAs epitaxial layer; before ELO band bending at the AlAs-GaAs interface accumulates this surface, while fermi level pinning depletes it for either an epitaxial

layer on SI GaAs or on quartz. After ELO, comparing backside and front side illumination, backside illumination shows a larger insertion loss and phase shift for the same illumination intensity.

Fig. 5.11 : Change of insertion loss at different illuminating conditions. Ground planes are reverse biased at 20 volts with respect to center conductor and laser optical intensity is kept at 0.65 mW/cm^2 . Δ : after ELO, unilluminated; \circ : after ELO, illumination from front; \diamond : before ELO, unilluminated; \blacktriangle : after ELO, illumination from back; and \blacklozenge : before ELO, illumination from front. Measurements are done on #1229 sample.

Fig. 5.12 : Change of n_{eff} at different illuminating conditions. Ground planes are reverse biased at 20 volts with respect to center conductor and laser optical intensity is kept at 0.65 mW/cm^2 . \circ : after ELO, illumination from front; \blacktriangle : after ELO, illumination from back; and \blacklozenge : before ELO, illumination from front. Measurements are done on #1229 sample.

Fig. 5.13 : Performance of an optically-controlled phase shifter (in terms of dB loss per degree of phase shift). Ground planes are reverse biased at 20 volts with respect to center conductor and laser optical intensity is kept at 0.65 mW/cm^2 . ○ : after ELO, illumination from front; ▲ : after ELO, illumination from back; and ◆ : before ELO, illumination from front. Measurements are done on #1229 sample.

These effects are mainly attributed to the lack of CPW electrode shadowing when the device is illuminated from the back, resulting in a larger absorbed optical power. The important figure of merit, loss figure (insertion loss per degree of phase shift) for three different situations (before ELO; after ELO front side illumination; after ELO back side illumination) is shown in Fig. 5.13. The larger phase shift from backside illumination (compared to frontside) is almost exactly compensated by the larger loss, producing nearly identical loss figures for both front and back side illuminations.

Fig. 5.14 : Performance of an optically-controlled phase shifter (in terms of dB loss per degree of phase shift). Positive bias corresponds to ground planes reverse bias whereas negative voltage means center conductor reverse-biased. Laser optical intensity with OD0 is 65 mW/cm^2 and with OD 2 is 0.65 mW/cm^2 . Measurements are done on #1675c sample.

With the sample #1675c ($3 \text{ }\mu\text{m}$ of epitaxial GaAs with a doping concentration of $5 \times 10^{15} /\text{cm}^3$ on the top of 500 \AA of AlAs and SI GaAs substrate), some optical measurements have been done with different biasing conditions, all of them before ELO. Fig. 5.14 shows the loss figures for two different illuminating intensities, both with center conductor reverse biased (-28 V) or ground planes reverse biased ($+28 \text{ V}$). Two different intensities were obtained using neutral density filters. It is evident from the figure that the ground planes reverse-biased situation gives better performance than center conductor reverse biased case. Fig. 5.15 shows the variation of loss figure when all three conductors are reverse biased with respect to a separate ohmic contact at three different illuminating intensities. In this case the sample is kept at a fixed bias of 25 V . Highest optical power (65 mW/cm^2) gives the best performance in this case.

With the sample #1946b (1.5 μm of epitaxial GaAs with a doping concentration of $5 \times 10^{15} / \text{cm}^3$ on the top of 500 \AA of AlAs and SI GaAs substrate) careful studies have been made at different biasing voltages to determine the optimum bias point for optical control of the device. At each voltage, the phase shift and the insertion loss were measured for the unilluminated and illuminated conditions, and then the loss figure (LF) was found using eqn. (5.3.1). The results of the studies are shown in Fig. 5.16. As an optical source, a broadband microscope illuminator was used for this study. In Fig. 5.16, positive voltage stands for ground planes reverse biased whereas negative voltage means the center conductor reverse biased.

Fig. 5.16 : Change of Loss Figure (LF) at different bias conditions (for both bias polarities) at a fixed frequency of 15 GHz.

From Fig. 5.16, it is evident that +4.5 volt gives the best optical performance. Based on this observation, subsequent optical-control measurements with a laser source are done with the ground planes kept at a fixed reverse bias of 4.5 volts. Different neutral density filters (OD 0, OD 1, OD 2, OD4) are used to vary the optical intensity of the laser, where the OD 0 (i.e., no OD) measures 65 mW/cm³ of power at the device surface.

Fig. 5.17(a) : Change of insertion loss at different illuminating conditions. Ground planes are reverse biased at 4.5 volts with respect to center conductor and laser optical intensity with no OD is kept at 65 mW/cm². ▲ : unilluminated; ● : laser with OD 4; ■ : laser with OD 2; ► : laser with OD 1; ◆ : laser with no OD. Measurements are done on #1946b sample.

Figure 5.17(a), (b) and (c) show the insertion loss, phase shift and loss figure respectively at different optical intensities, all kept at fixed reverse bias of +4.5 V. From Fig. 5.17(c), it is shown that at higher than a certain optical intensity (in this case OD 4) loss figure becomes close to identical. With all these data, all before

ELO, none of the loss figure performance matches the best result of a epitaxially lifted off sample.

Fig. 5.17(b) : Optically-induced phase shift at different illuminating conditions. Ground planes are reverse biased at 4.5 volts with respect to center conductor and laser optical intensity with no OD is kept at 65 mW/cm². ● : laser with OD 4; ■ : laser with OD 2; ► : laser with OD 1; ◆ : laser with no OD; Measurements are done on #1946b sample.

With the sample #2299a (2 μm of epitaxial GaAs with an n type doping concentration of 5 x 10¹⁵ /cm³ sitting on the top of 500 Å of AlAs and SI GaAs substrate combination), optical measurements have been done at different biasing voltages to find the optimum voltage for optical control.

Fig. 5.17(c) : Performance of an optically-controlled phase shifter (in terms of dB loss per degree of phase shift). Ground planes are reverse biased at 4.5 volts with respect to center conductor and laser optical intensity with no OD is kept at 65 mW/cm². ● : laser with OD 4; ■ : laser with OD 2; ► : laser with OD 1; ◆ : laser with no OD. Measurements are done on #1946b sample.

From the experiment, +6 V or +7 V came out to be the optimum voltage for optical control measurements. Just for a comparison, in Fig. 5.18, loss figures are shown for both bias polarities at -7 V (center conductor reverse biased) and with +7 V (ground planes reverse biased) at two different optical intensities (laser with OD 1 and OD 2). With ground planes reverse biased the loss figures tend to remain flat over the wide frequency range of 5 GHz - 40 GHz. This makes the device a viable candidate for the practical implementation of a millimeter wave phase shifter for commercial applications, which requires a very small optical power and a

comparable (with other commercially available microwave phase shifter) figure of merit (loss figure) performance, as discussed in the next section.

Fig. 5.18 : Performance of an optically-controlled phase shifter (in terms of dB loss per degree of phase shift). Positive and negative voltage mean ground planes and center conductor reverse biased both at 7 volts. Laser optical intensity with no OD is kept at 65 mW/cm². ○ : - 7 volts, laser with OD1; ▲ : + 7 volts, laser with OD2; and ◆ : + 7 volts, laser with OD1. Measurements are done on #2299a sample.

5.4 : Comparison with other phase shifters

A number of attempts have been made to fabricate a good phase shifter in the microwave and millimeter wave frequencies, employing Schottky optical [Lee et al. 1980; Vaucher et al. 1983; Cheung et al. 1985; Lin et al. 1987; Platte 1989]

using Schottky-contacted microstrip or CPW conductors. Most Schottky-contacted voltage controlled microwave devices [Krowne et al. 1986; Krowne et al. 1987]

with high doping concentrations, insertion loss is also very high. Also fabricating a Schottky contact on the heavily doped materials is not easy and usually requires complex processing steps. Use of optical illumination to make a phase shifter was first demonstrated by Chi H. Lee

in a waveguide and showed that at a very high plasma density, a large phase shift can be achieved

in an optically controlled phase shifter. They made a hybrid phase shifter using lateral p-i-n diodes monolithically integrated into a CPW structure. These p-i-n diodes act as a lumped circuit loading of the CPW; a logical extension would be a distributed Schottky line to form the CPW [Cheung et al. 1989; Kaiser et al. 1989]

rather than a voltage controlled one, and that is why it required very intense optical source.

Combining both Schottky and optical control a phase shifter was made on a quartz substrate (after the ELO process), which shows

better performance

frequency is increased (at least up to 40 GHz). This shows the promise of using the GaAs-on-Quartz phase shifter in the millimeterwave regime and still obtaining similar performance. Table 5.1 shows the performance of several reported phase shifters, which as well includes a list of a few commercially available electronically-controlled phase shifters. To date, no commercial phase shifter has been found which operates above 18 GHz. The loss figures quoted for most of the other phase shifters show better performance characteristics at or below 18 GHz. But, all these mechanisms are sure to degrade at higher frequencies. Whereas, the ELO Schottky-contacted optically-controlled phase shifter showed similar performance up to 40 GHz range.

Table 5.1 : Comparison with other phase shifters

No.	Device description	Controlling mechanism	Frequency range	Loss figure	Reference
-----	--------------------	-----------------------	-----------------	-------------	-----------

1	Schottky on GaAs	Optical	1-40 GHz	0.14@30GHz 0.11@10GHz	Cheung
2	Schottky on Si	Voltage	1-20 GHz	0.083@20GHz	Champlin[Hi etala et al. 1987]
3	Schottky μ strip GaAs	Voltage	dc - 18GHz	0.2@2GHz 0.16@10GHz 0.08@18GHz	Krowne[Krowne et al. 1986]
4	Schottky on GaAs	Optical	1-8 GHz	no insertion loss data given	Jager[Kaiser et al. 1989]
5	GaAs MMIC circuit	Voltage	8-12 GHz	0.12@12GHz	Frost
6	Commercial analog phase shifter	Voltage	8-18 GHz	0.042@8-18GHz	KDI Triangle
7	Commercial analog phase shifter	Voltage	8-18 GHz	0.067@8-18GHz	General Microwave
8	Commercial analog phase shifter	Voltage	dc-18GHz	-	M/A Com
9	Commercial analog phase shifter	Voltage	dc-18GHz	-	Hughes
10	Schottky on ELOed GaAs	optical	dc - 40GHz	0.1@1-40GHz	Islam[Islam et al. 1991]

5.5 : LED-controlled millimeter wave 90° Phase shifter

It has already been shown that Schottky-contacted coplanar waveguide (CPW) on GaAs substrates produce large phase shifts of microwave signals when

the substrate is optically illuminated, even at very low illumination intensities here the original semi-insulating GaAs substrate is replaced by an optically transparent, low dielectric constant quartz substrate. A millimeter Wave (20 GHz - 40 GHz) 90° phase shifter was implemented where the illumination source was a common commercially available plastic-encapsulated red LED.

5.5.1 : Device Fabrication:

The original CPW phase shifter substrate consists of an epitaxial layer of 3 μm thick lightly-doped n-type ($\sim 5 \times 10^{15} \text{ cm}^{-3}$) GaAs grown on a semi-insulating (SI) (100)-oriented GaAs wafer, with a 500 Å AlAs release layer sandwiched between the active layer and the substrate. CPW electrodes are then fabricated on the GaAs-AlAs-SI GaAs substrate combination. The CPW electrodes consist of 100 Å of evaporated chrome, 200 Å of evaporated gold, and 1 μm of electroplated gold. The center conductor of the CPW is 10 μm wide, and the gaps to the ground planes are 7 μm. To remove the epitaxial layer and CPW from the SI substrate the

AIAs release layer is selectively etched away and the thin epitaxial layer is

5.5.2 : Device Operation and Performance:

Maximum sensitivity to optical illumination is obtained when a dc reverse bias is applied to the CPW electrodes that just depletes the epitaxial layer under the metal at zero illumination intensity. At this dc bias very low levels of illumination induce large changes in the CPW transmission line admittance per unit length, with which [1978]

, as explained in Chapter 4. For the doping concentration and the layer thickness of the device used, a reverse bias of 29 V applied to the ground plane conductors with respect to the center conductor produced maximum sensitivity. At this bias and at zero illumination intensity, the propagation constant and characteristic impedance of the CPW is approximately that of a CPW on a lossless substrate. The CPW phase shifter was illuminated with an inexpensive (present cost US \$1 - \$2) commercially available epoxy-encapsulated red LED ($\lambda = 0.6 \mu\text{m} - 0.75 \mu\text{m}$). The LED is placed just underneath the quartz substrate providing back side illumination of the GaAs, thus allowing higher light absorption in the active GaAs layer (as shown in Fig. 5.19). The LED used can produce $\sim 190 \mu\text{W}$ of optical power at a dc power level of 87 mW; this LED setting was the maximum optical power used to produce phase shift over a 20 GHz - 40 GHz frequency range. The optically-induced phase shift and the insertion loss of a 1 cm long CPW were measured with an HP 8510B automatic network analyzer and wafer probes.

Fig. 5.19 : Experimental arrangement of back side illumination of an ELO-ed GaAs-on-Quartz phase shifter with a commercially available red LED.

Based on the measured phase shift per centimeter at maximum illumination intensity, the length of a device designed to produce a specific phase shift can be calculated. For example, the length for a 90° phase shifter is shown in Figure 5.20. For such a 90° phase shifter, the optically induced phase shift and the insertion loss as a function of LED optical output power are shown in Figures 5.21 and 5.22, respectively. At 35 GHz, a 90° phase shifter would be about 3.5 mm long, with about -11 dB of insertion loss at 90° phase shift (for maximum LED illumination intensity used), and about -4 dB of loss at 0° phase shift (for zero illumination intensity). The simple structure and the inexpensive optical source used in this case make this device a potential candidate for commercial application as a phase shifter. The very high optical sensitivity exhibited by the GaAs-on-quartz CPW is critical to the development of practical optically-controlled microwave components.

Fig. 5.20 : Length required for a LED-controlled phase shifter to produce 90° phase shift.

Fig. 5.21 : Variation of insertion loss of an LED-controlled 90° phase shifter with changing frequency and input dc LED power.

Fig. 5.22 : Optically-induced phase shift of an LED-controlled 90° phase shifter as a function of operating frequency and input dc LED power.

Fig. 5.23 : A CPW phase shifter and a double heterojunction LED are epitaxially lifted off onto both sides of a same quartz substrate to implement an integrated LED / Phase shifter.

Using the ELO process, it should also be possible to integrate a simple GaAs-AlGaAs double-heterojunction (D-H) LED with the phase shifter using both sides of the quartz substrate, as illustrated in Fig. 5.23. With direct bonding of the LED opposite the CPW phase shifter, much higher optical coupling efficiency

should be realized. Such an integrated LED / phase shifter should require much lower dc drive power for the optical source, making the control of the device extremely simple.

5.6 : Pulse response measurements of the phase shifter

It has already been shown in the earlier sections that a microwave signal carried on a Schottky-contacted co-planar waveguide (CPW) on a GaAs substrate can undergo large phase shifts when the substrate is optically illuminated even at very low illumination intensities. Past experiments have been made only for continuous (CW) illumination of the CPW. However, the response of the device to time-varying optical illumination is of great importance for microwave and optoelectronic applications where dynamic operation is required. In this section a preliminary measurement of response times of an optically illuminated CPW phase shifter is presented. Results indicate the possible presence of optically active semiconductor trap states with extremely slow response times, which can dominate the microwave propagation characteristics of the CPW. A possible way to prevent this "optical back-gating" effect is also discussed.

5.6.1 : Experimental set-up

To measure the response time of the device, a modulated laser diode array was used for the illumination source, operating at a wavelength of 809 nm, which is shorter than the bandgap of GaAs. The pulse repetition rate of the laser was varied between 400 Hz and 1 kHz. The rise and fall time of the driving current pulse for the laser was in the range of 100 nsec. The optical pulse length was varied between 100 μ sec and 400 μ sec. Neutral density filters were used to adjust the illumination intensity to achieve various amounts of phase shift. The device was held at a fixed DC bias, with the center conductor reverse biased. An electromagnetic wave from an oscillator was passed through the device, and the change in phase and attenuation due to the modulated optical source was monitored. Figure 5.24(a) & 5.24(b) show the insertion loss and phase shift measured with a conventional

Network Analyzers, a function of CW illumination intensity . The plots show the non-linear response of the device to intensity changes. In dynamic operation this would be expected to produce some slight differences between illuminator switching speed and device switching times. The experimental set-up for the pulsed measurements is shown in Fig. 5.25. Connection to the CPW device was made using Design Technique RF wafer probes. The RF signal used for the experiment was varied over the range of 8 - 12 GHz. The CPW was kept at a fixed

ed current were also monitored using an oscilloscope.

Fig. 5.24(a) : Insertion loss performance at different CW illuminating intensities measured for pulse response evaluation.

The RF system shown in Fig. 5.25 acts as an interferometer, producing an IF mixer output which is dependent upon the optically-induced change in the amplitude and phase of the signal propagated through the CPW. Depending on the initial phase difference between the arms of the interferometer, maximum sensitivity to phase or amplitude change can be achieved. A second set up used a simple square-law microwave power detector (eliminating the power divider, reference arm, and mixer) to measure only the change in amplitude of the signal. Because the mechanism which generates phase change is integrally associated with changes in attenuation constant for the CPW, the time constant for the two effects should be similar. In practice, it is usually easier to monitor the time constant of amplitude changes for these devices, since the change in insertion loss between light-on and dark states is fairly large.

Fig. 5.24(b) : Phase shift performance at different CW illuminating intensities measured for evaluating pulse response.

5.6.2 : Results and discussions

At 8 GHz a phase shift of 65° and insertion loss of -10 dB were achieved at a laser output of 60 mW/cm^2 (peak power). The rise time (time from light pulse on to steady-state light-on condition) was quite fast, with an exponential time constant of about 50 μsec . However, the transition from light-on state to light-off state was

Fig. 5.25 : Block diagram of rf system set up to measure the pulse response time of a CPW phase shifter

extremely slow. For the GaAs epi-layer directly on the top of semi-insulating (SI) GaAs substrate, the on-off transition was approximately exponential, with time constant of about 2 msec. In contrast, the photo-generated current monitored in the bias network had both rise and fall time constant of about 50 μsec . This was consistent with the RC time constant associated with the measured low-frequency capacitance and internal resistance (about 100 pF and 100 k Ω) of the CPW "photo-diode".

It is clear from these results that there is some extremely slow optically-induced effect which dominates the rf characteristics of the CPW, but does not directly influence the photo-generated current produced. For a room temperature semiconductor device, only trap states are normally found to exhibit such long time constants. A possible explanation for the behavior of this device is that the charge states of the traps somewhere in the GaAs substrate is altered when it is illuminated. The change in charge state alters the electrostatic fields in the device, and thus the width of the depletion layers. This in turns determines the microwave

propagation constant of the CPW. When the light is turned off, if the trap transition times are long, the widths of the depletion layers can only move slowly back to their light-off positions. The photo-generated current, however, is determined primarily by the number of photons absorbed per unit time during the laser-on period; so long as the trap concentration is not too large, the photo-current in the bias circuit should approximately follow the light pulse.

The traps discussed above may reside at the metal-semiconductor interfaces, in the epi-layer itself, at the epi-SI substrate interface, or in the bulk SI GaAs substrate. To help identify the location of the traps a CPW on an n-type GaAs/AlAs/SI GaAs substrate was also tested. This device showed even slower response, with a light-on to light-off transition time of more than 70 msec. The time constant for the photo-current is still in the range of 10-50 μ sec. This may indicate that the traps are located at the interface just below the n-type epi-layer.

The slow transient effect in epitaxially grown GaAs on SI substrate has also been reported previously. It can also be activated with optical illumination and thus causing a long term transient effect.

5.6.3 : Conclusions

Based on the results of the pulsed illumination experiments, it would appear that slow semiconductor traps may have a strong influence on the microwave propagation constant of these optically-controlled CPW phase shifters. In order to increase the speed of the device it is necessary to eliminate the traps. This would also be expected to change the overall optical sensitivity, since CW measurements to-date have been made on samples dominated by trap effects. However, optically-induced changes in depletion layer thickness, and therefore, in surface sheet resistance of the back substrate are well documented in other semiconductor devices, so phase shift in CPW should still be achieved. One potential way to reduce interface traps and substrate related effects is through the use of a GaAs

buffer layer grown at very low temperatures (LT GaAs) between the active n-type GaAs epi layer and the SI GaAs substrate. However, if the traps are located at the surface of the active layer,

layer thickness and doping, may allow the fabrication of a Schottky-biased optically controlled CPW phase shifter which exhibits both high optical sensitivity and high speed and which might find a place in commercial application of broadband phase shifter.

5.7 : Summary :

In this Chapter, experimental characterization of voltage and optical control CPW phase shifters are discussed in detail. All the measurements were performed up to 40 GHz using the Network Analyzer. The figure of merits of the phase shifters were computed and compared with other available phase shifters; and it was found that the ELO phase shifter had the best performance of all. A 90° millimeter wave phase shifter was implemented using a commercially available red LED. The possibilities are also discussed to design an integrated LED-phase shifter on the same quartz substrate keeping similar to better performances. Furthermore, a preliminary measurement is performed to calculate the response times of the phase shifter to the pulsed illumination.